Environmental Science Nano

Accepted Manuscript

ROYAL SOCIETY OF CHEMISTRY

rsc.li/es-nano

This report describes the distribution and retention of several nanocerias after their systemic administration to rats. The results are compared to reports of the same endpoints after systemic administration of higher doses of the same nanoceria, and different nanoceria, and indicate the lack of great differences in the distribution and retention of nanoceria as a function of dose, size, shape, or dosing schedule. The results inform about the sites of nanoceria accumulation in mammals and the duration of persistence at those sites. The similarity of nanoceria distribution following systemic administration of different sizes, doses, shapes, and dosing schedules leads to a summary understanding of nanoceria's fate when introduced into the blood, for example as a therapeutic agent.

Journal Name

RSCPublishing

ARTICLE

Nanoceria biodistribution and retention in the rat after its intravenous administration are not greatly influenced by dosing schedule, dose, or particle shape

Cite this: DOI: 10.1039/x0xx00000x

Received 00th January 2012,
Accepted 00th January 2012

DOI: 10.1039/x0xx00000x

www.rsc.org/

Robert A. Yokel[a,b], Jason M. Unrine[c], Peng Wu[d], Binghui Wang[d], Eric A. Grulke[d]

A 30 nm ceria was previously shown to be primarily cleared from systemic circulation into mononuclear phagocyte system organs after its intravenous (IV) administration, where it persisted for 90 days. The aims of these studies were to determine if the biodistribution, persistence, and toxicity of nanocerias are affected by dosing schedule, dose, or particle shape. Given the many demonstrated and ongoing uses of nanocerias; the multitude of applications under investigation; and the many sizes, shapes, and surface functionalizations of ceria; a better understanding of its fate is necessary to advance its safe use. Five and 30 nm cubic/polyhedral ceria and a ceria nanorod (9.9 x 264 nm average diameter and length) were IV infused into rats once. The 5 nm ceria dose was also infused daily for 5 consecutive days. The rats were terminated 1 h to 90 days later. Cerium was determined in multiple organs and blood. Compared to vehicle-infused controls, elevated cerium was seen in all sites. Liver, spleen, and bone marrow (mononuclear phagocyte system components), contained the largest percentage of the dose. When normalized to dose, and compared to results of prior work with these nanocerias, the distribution and retention of repeated and lower doses of 5 and 30 nm ceria and ceria nanorods were not greatly different from much higher doses of the 5 and 30 nm ceria. Higher doses resulted in a greater percentage of uptake by the spleen and bone marrow and a greater percentage of the ceria nanorod dose in the bone marrow 30 days after its administration than the other nanocerias. Overall these results suggest the biodistribution and retention of cerium after IV administration of different sizes, doses, dosing schedules, and nanoceria shapes are more similar than different.

Introduction:

There is much interest in nanoscale ceria (a.k.a.: CeO_2, cerium dioxide) particles because they are being used and pursued for multiple applications. Nanocerias have auto-catalytic oxidation/reduction properties; the ability to self-assemble; the presence of oxygen vacancies; are quite insoluble and abrasive; and their synthesis can be tuned to modify size, structure, and substitutional lattice doping properties. Capitalizing on these properties, they are used as a catalyst in the water gas shift reaction for fuel cell power generation; in catalytic converters; and in fuel borne additives to catalyze combustion, decrease combustion temperature, and decrease fouling [1]. The main current use is as an abrasive catalyst in chemical mechanical planarization/polishing in silicon integrated circuit fabrication. Nanocerias are expected to have future application in fuel cells and batteries. Due to their autocatalytic behavior, i.e., their ability to reduce reactive oxygen and nitrogen species, nanocerias have been shown to protect against cytotoxicity induced by H_2O_2 and nitric oxide [2-6], diesel exhaust particles [7], radiation [8-10], glutamate [11], Aβ protein [12], ischemia [13], and reactive oxygen species-induced by lipopolysaccharide/IFN-γ [14] and cigarette smoke [15]. Nanocerias protected against H_2O_2-induced apoptosis [16], enhanced rat spinal cord neuron viability in the absence of intended stress [17], reduced reactive oxygen species in a mouse knockout model of retinal neovascular lesions [18], and reduced the clinical effects of a murine model of multiple sclerosis [19]. Nanoceria efficacy has been shown in models of cardiomyopathy [20], ventricular hypertrophy [21], cancer [3, 22, 23], ischemic stroke [24], and hypobaric hypoxia [25], and as an antibacterial and antifungal [26, 27] and radioprotective agent [8-10]. However, there is concern about the potential toxicity of nanocerias, which are quite insoluble [28, 29] and persist in the organism [19, 28, 30-35]. Nanocerias have been reported to produce adverse effects *in vivo* and *in vitro*, including decreased viability and DNA content in 3T3 rodent fibroblast and MSTO-211H human mesothelioma cells [36]; decreased viability, death, and induction of oxidative stress-related genes in BEAS-2 human bronchial epithelial cells [37, 38]; increased neutrophils and inflammatory cytokines in the bronchoalveolar fluid and formation of lung granulomas in mice [39]; increased oxidative stress in the lung of rats after inhalation exposure [40]; pulmonary inflammation and fibrogenic responses in rat lung after intratracheal instillation [41, 42]; microvascular dysfunction [43];

Kupffer cell activation, formation of granuloma, hydropic degeneration of hepatocytes, dilation of the sinusoids, portal inflammation, and fibrosis in the liver of rats [30, 31, 44-46]; and increased oxidative stress in the brain [30, 47, 4849] and liver and spleen of rats after intravenous (IV) administration [31, 44].

The IV route has been studied to characterize the fate of nanocerias in systemic circulation after translocation from the site of uptake, such as the lung. This route is also relevant as a benchmark for comparison to the fate of nanocerias by non-systemic routes of exposure because the IV route provides 100% bioavailability. It is also relevant to, and might be necessary for, the proposed use of nanocerias as therapeutic agents. Nanocerias have low bioavailability from the lung and gastrointestinal tract. To achieve the concentrations at the site of its intended effect (as demonstrated in *in vitro* studies) [32] requires nanoceria introduction at its target site or possibly by systemic administration. Uptake of a 7 nm ceria from the lung after intratracheal instillation resulted in translocation of only ~ 0.1, 0.01, 0.001, 0.0001 and 0.00001% of the dose to the liver, spleen, kidney, heart and testes, and brain 28 days later, respectively [28]. Uptake from the gastrointestinal tract is even lower. Oral administration of the same 7 nm ceria resulted in ~ 0.0001% of the dose in the liver and lower amounts in the brain, heart, kidney, lung, spleen, and testes 1 to 7 days later [28]. A single oral administration of a 30 nm ceria, 100 mg/kg, resulted in ~ 0.015, 0.003, 0.002, 0.0012, 0.0012, and 0.0006% of the dose in the liver, testes, lung, kidney, brain, and spleen, respectively, 14 days later [35]. When 0.5 mg/kg crystalline, carboxyfluorescein-functionalized 3 to 5 nm primary particle size 15 to 20 nm agglomerate ceria particles were given orally to CD-1 mice weekly for 2 or 5 weeks, ~ 0.2% of the dose was in the lung (that was most likely due to the gavage procedure or aspiration); 0.025% in the spleen; less in the liver, kidney and heart; and none was detectible in the brain 1 week later [33].

Limited results suggest that the number of nanoceria administrations does not greatly affect its fate. One week after 2 or 5 weekly IV injections of 0.5 mg/kg of the carboxyfluorescein-functionalized 3 to 5 nm primary particle size ceria (above paragraph) were given to CD-1 mice, organ cerium concentrations were about 3 times higher in the mice that received 5 vs. 2 injections [33, 50]. Approximately 37, 3, 0.15, and 0.008% of the dose was in the liver, spleen, lung, and kidney, respectively. None was detectible in the brain.

Nanoceria has multiple current uses, there are many human conditions it has been shown to effectively address, and it is being, and will be, investigated for further applications. Many sizes, shapes, and surface functionalizations of nanoceria are being utilized and investigated. Some of these uses will probably require systemic administration to treat diseases, given the very low absorption from the gastrointestinal tract and lungs. The distribution and persistence of several sizes of cubic/polyhedral nanoceria have been described in the rat after its single systemic administration, often utilizing very large doses [30-32]. Further work is needed to understand if these prior findings can be generalized, e.g. to lower exposures, other shapes, and repeated exposure. The objectives of the present research were to determine if the biodistribution and persistence of nanocerias are different following lower doses than used in many of the above studies and if repeated dosing and particle shape influence their disposition and retention. To ascertain the fate of nanocerias after repeated exposure, the 5 nm ceria was infused daily for 5 consecutive days (11 mg/kg/day) and the rats terminated 30 days later. To determine if the nanoceria dose greatly affects its fate, 11 mg/kg of a 5 nm polyhedral ceria and 6 mg of a 30 nm cubic ceria were intravenously infused into rats that were terminated 30 and up to 90 days later, respectively. The results were compared to prior work using the same nanoceria and procedures, but a dose of 85 mg/kg [31, 32]. A ceria nanorod (average diameter and length: 9.9 and 264 nm) was given once by IV infusion (20 or 50 mg/kg) to rats that were terminated 1 h or 30 days later, to be able to compare its distribution and retention to cubic/polyhedral ceria.

It is expected that the behavior of these quite insoluble metal-based nanomaterials *in vivo* over time would be informative of the behavior of other quite insoluble nanomaterials composed of metals that are not rapidly eliminated from the mammalian organism.

Methods:

The nanocerias studied:

Synthesis and characterization of the citrate-capped 5 and 30 nm nominal diameter polyhedral/cubic ceria have been described [32, 44, 51]. Their physical-chemical properties are shown in Table 1.

	5 nm ceria	30 nm ceria	nanorod
Average primary particle size by TEM, in nm (Sauter mean diameter)	4.6 (4.8)	31.2 (51)	Average diameter 9.9 ± 2.0 and length 264 ± 112.
BET surface area, in m^2/g (and corresponding diameter, in nm)	121 (6.5)	15 (52)	54 (estimated from diameter, length & density)
DLS hydrodynamic diameter (volume-average[a]) in nm	7	41	Bimodal: 100 nm (5%); 400 nm (95%)[b]
Zeta potential (pH 7.3 in water), in mv	-53	-56	-25[c]
Extent of citrate coating, as percent of monolayer[d]	~ 40	~ 18	~100
Miller indices of the most common faces	(111)(210) (200)	(200)	(111)(200) (220)

Table 1. Physical-chemical characteristics of the nanocerias studied. [a] – Volume (mass)-based particle size, reported here, is directly linked to biological or environmental exposure. [b] – measured on the original sample that was stored three years in 10% sucrose suspension. [c] – An experimental study of zeta potential measurements on short nanorods (L/D ~ 4) showed that their expected hydrodynamic diameter was 10% higher than that of spherical particles [52]. This correction was applied to the obtained DLS results. [d] – Area-equivalent diameter of citrate acid as 0.36 nm, close-packed adsorption on the nanoparticle surface. Citric acid is thought to associate with polar surface groups, such as hydroxyls, which might explain its high surface coverage on the nanorods (relative to the spheroidal nanoparticles).

The nanorod ceria was synthesized following a published method and characterized in house [53]. Cerium (III) nitrate hexahydrate (2.17 g) (Fluka, CAS # 10294-41-4) was dissolved into 12.5 ml water, then stirred for ~5 min. Sodium hydroxide (31.5 g) was dissolved into 87.5 ml water and was stirred for 10 min (9 M). The cerium nitrate solution was added into the sodium hydroxide solution drop wise with continual stirring for 30 min. The mixture was transferred into a large capacity acid digestion bomb (~125 ml, 80% occupied, Model 4748, Parr Instrument Company) and heated at 100 °C for 24 h. It was then cooled at room temperature. The product was washed with water 3 times and ethanol twice, then dried in an oven at 65 °C overnight.

The dimensions of the ceria nanorods were determined from images of 102 nanorods visualized by a 200-kV field emission analytical transmission electron microscope (TEM) (Figure 1). The specific surface area (SSA) was measured by the BET method. The BET tubes with sample were heated up to 120 °C for 4 h to remove water and gas. No water droplets were found on the glass wall after the heat treatment. The hot tubes were purged with nitrogen gas and cooled to room temperature. X-ray diffraction (XRD) was used to characterize the crystal structure of the ceria nanorod sample. The dry ceria powder was dispersed in ethanol. Some drops of dispersion were placed on a glass slide. After the ethanol evaporated, the remaining ceria thin film was characterized by XRD. Results of its characterization are shown in Table 1.

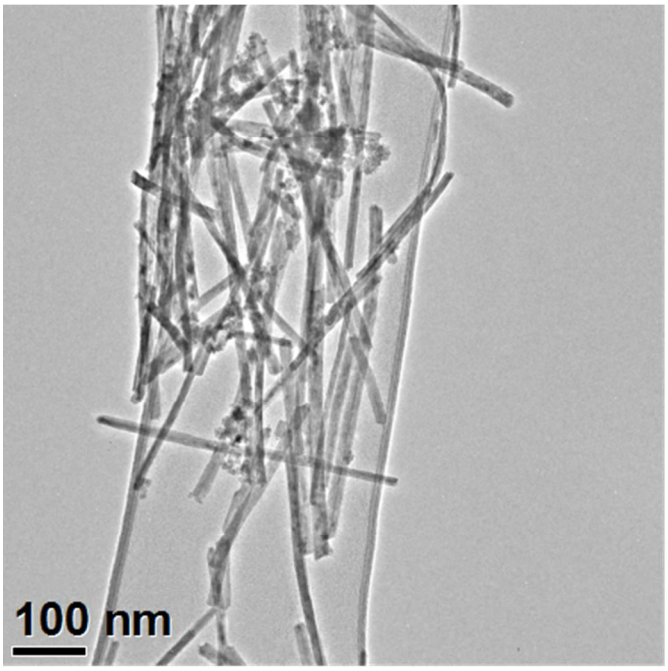

Figure 1. Transmission electron microscopic image of the ceria nanorods.

Citric acid was used to maintain a good dispersion of synthesized ceria nanorods since it can supply a negative charge on nanoceria's surface [54]. Dried ceria nanorods (0.5 g) were dispersed in 50 ml of aqueous solution containing 0.6 g citric acid. The dispersion was stirred for 24 h to thoroughly adsorb the citric acid on the nanoceria's surface. The product was washed with water 5 times to remove any free citric acid, and then dried in an oven overnight at 65°C. The dried sample was dispersed in 10% sucrose solution by sonication for 10 min and was infused into the rats.

Animals:
This study reports results from 67 male Sprague Dawley rats, weighing 386 ± 58 g (mean ± SD) (~ 90 days old). Procedures to prepare the rats for IV nanoceria infusion, organ and blood collection, processing procedures, and cerium quantification methods have been described [30, 32]. The rats were infused when not anesthetized to enable observation of effects produced without the confounding effects of anesthesia. The 5 and 30 nm ceria were infused in water to avoid agglomeration. A concurrent infusion was given of 1.8% sodium chloride at the same rate in a second IV cannula to deliver a net isosmotic load to the rat. All nanoceria dispersions were infused at a rate of 2 ml/kg rat body weight over 1 h, with the exception of the 50 mg/kg dose of nanorods, which was infused over 2.5 h. The rats were obtained from Harlan, Indianapolis, IN. They were housed individually prior to study and after cannulae removal (a few days after the IV infusion) in the University of Kentucky Division of Laboratory Animal Resources facility under a 12:12 h light:dark cycle at 70 ± 8°F and 30 to 70% humidity. The rats had free access to 2018 Harlan diet and reverse osmosis water. Animal work was approved by the University of Kentucky Institutional Animal Care and Use Committee. The research was conducted in accordance with the Guiding Principles in the Use of Animals in Toxicology (http://www.toxicology.org/ai/air/air6.asp).

Treatment groups:
Five rats were infused with 11 mg/kg of the 5 nm ceria once, 5 with 11 mg/kg of the 5 nm ceria on each of 5 consecutive days for a total of 55 mg/kg, and 5 received vehicle infusion. All were terminated 30 days later. Rats were infused with 6 mg/kg of the 30 nm ceria along with controls which were infused with vehicle, and 5, 4, and 5 treated and 3, 4, and 3 controls terminated 1 h, 30 days, and 90 days later, respectively. In initial studies, two un-anesthetized rats were IV infused with ~ 50 or 100 mg/kg nanorod ceria over 2.5 or 5 h. The 50 mg/kg dose was tolerated but the rat that received 100 mg/kg was slow, weak, and not responsive to a cage tap. Therefore, the test dose was 50 mg/kg nanorod ceria infused IV over 2.5 h. Nine rats were infused with 50 mg/kg of the ceria nanorod. Five rats were terminated 1 h and 4 rats terminated 30 days later. Five rats infused with 20 mg/kg of the ceria nanorod were terminated 30 days later. Paired with the rats that received the ceria nanorod infusion were 5 vehicle-infused control rats terminated 1 h and 5 terminated 30 days later.

Sample collection, processing, and cerium analysis:
Samples were harvested on termination from the organs and blood shown in Figures 3, 4, and 5 following described procedures [31]. Additionally, mesenteric lymph nodes and fat were harvested from some rats, as nanoceria deposition to these sites has not been previously reported to our knowledge. Samples were prepared and analyzed for cerium by microwave-assisted nitric acid/hydrogen peroxide digestion and inductively coupled plasma mass spectrometry (ICP-MS), as described [30]. The method detection limits (MDL) were 0.089 mg Ce/kg for tissues and 0.018 mg Ce/l in blood samples. Spike recovery for ICP-MS analyses was 94 ± 3% (mean ± SD). Average relative percent difference between replicate analyses was 3.2 ± 2.0% [30].

Data and statistical analysis:
Cerium concentrations below the MDL were assigned 50% of the MDL and included in the statistical analysis as such. The percentage of the nanoceria dose in the adrenal and thymus glands, brain, heart, kidney, liver, lung, and spleen was calculated as cerium concentration in the analyzed sample multiplied by the weight of the organ, as harvested, divided by the nanoceria dose. The nanoceria dose was determined as the cerium concentration in the dosing dispersion (determined by ICP-MS) times the dose volume. The percentage of the nanoceria dose in blood was based on a vascular volume of 7% of the rat's body weight [55]. The percentage of the nanoceria dose in the lymph node (0.4% of body weight) was based on the lymph nodes of the rat [56], weight of the mesenteric lymph nodes (0.3 gm) [57] and average weight (20 mg) of many other lymph nodes [58, 59]. The percentage of the nanoceria dose in other organs was based on reported values; bone marrow (3%) [60, 61], skeletal muscle (45%) [reference 20 in 62, 63], and fat (12.5%) [64-66].

Outliers in blood and tissue cerium concentration results identified by the Grubb's test (http://www.graphpad.com/quickcalcs/Grubbs1.cfm) were not used in data analysis. Results of control rats for blood and each organ were compared to the % of the nanoceria dose in treated rats by an unpaired one-tailed t test with Welch's correction, accepting significance when the alpha was less than 0.05/t, where t = the number of comparisons for that treatment. Results of nanoceria-treated rats were compared within blood or organs across termination times (for the 30 nm and nanorod ceria), and/or total dose (for the 5 nm and nanorod ceria), for each of the groups that received the same nanoceria, and across all treatments of this study plus our prior studies [31, 32] for liver, spleen and bone marrow by ANOVA with Tukey's post-hoc test or two-tailed unpaired t tests. Results are reported as mean ± S.D.

An analysis of the percent of the dose in each sampled organ compared to the percent that would be expected if the nanocerias non-selectively distributed, a relative deposition index as described by [67, 68] was conducted. Organ volumes were averages from our studies or those described above for blood, lymph node, bone marrow, skeletal muscle, and fat. By relating the amount in an organ to its size, this calculation identifies sites of preferential nanoceria accumulation.

Results:
A transmission electron microscopic image of the ceria nanorods is shown in Figure 1. The physical characterization of this sample was based on TEM analysis of 102 ceria nanorods. The average diameter and length of the ceria nanorods was 9.9 ± 2.0 nm and 264 ± 112 nm, respectively. As the nanorods grew from the cubic faces of (200) ceria nanocubes, and these nanocubes had a relatively narrow size distribution, the diameter distribution is also relatively narrow. The length distribution was quite broad, with $L_{0.10}$ = 120 nm, $L_{0.50}$ = 264 nm, and $L_{0.90}$ = 381 nm. All of the nanorods are considerably shorter than 1 μm. Their average aspect ratio (length/diameter, AR) was 27 ± 10 nm, with $AR_{0.10}$ = 14, $AR_{0.50}$ = 27, and $AR_{0.90}$ = 40. Analysis of two fields of ceria nanotubes to determine the relationship between diameter and length showed an inverse correlation of low significance (R^2 =0.20).

The ceria nanorod surface area per unit mass was estimated from the dimensions via the following calculation, which has been applied to estimate SSA for nanoparticles with different shapes like cubic ceria nanoparticles and graphite nanodisks [54, 69].

$$\mathrm{SSA} = \frac{\text{surface area}}{\text{weight}} = \frac{\text{surface area}}{\text{density} * \text{volume}} = \frac{\frac{\pi d^2}{2} + \pi dl}{\rho \frac{\pi d^2}{4} l} = \frac{2d + 4l}{\rho dl}$$

When the average d (9.9 nm), l (264 nm) and ρ (7.65g/cm^3) were used, the estimated SSA value was 53.7 m^2/g. The result was very close to the SSA measured by the BET method (52.7 m^2/g). This is intermediate between the SSA of the 15 and 30 nm ceria we previously studied [32], suggesting the ceria nanorods should have a similar biodistribution and retention behavior, unless these properties are influenced by shape.

The XRD pattern of ceria nanorods is shown in Figure 2. It demonstrates that the ceria nanorods were highly crystalline. The angle values of each peak were the same as the 5 nm and 30 nm ceria, although the peak shapes were not as sharp as those of the 5 nm and 30 nm ceria. The shape difference may arise from the substitution of peaks with different widths, which results from the wide distribution of nanorod length.

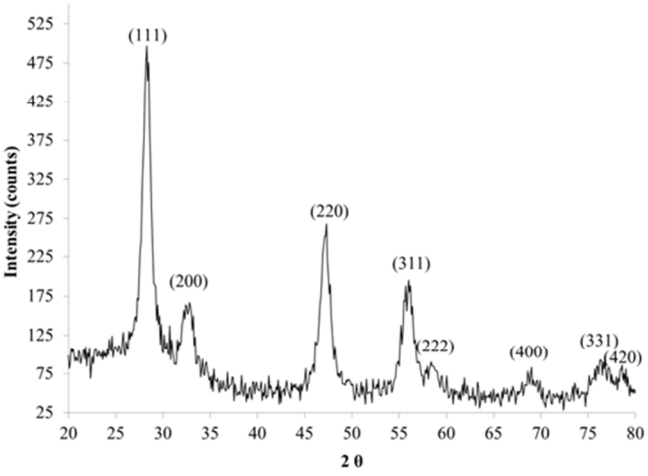

Figure 2. X-ray diffraction pattern of the ceria nanorod sample.

Of the 293 samples from control rats analyzed for cerium, 56 (19%) were above the MDL of 0.089 mg/kg for tissue and 0.018 mg/l for blood. These were most commonly in the liver, spleen, brain, bone marrow, bone, and lung. Twenty-three values from control subjects were outliers by the Grubb's test, mostly due to only one of the several subjects' values being above the MDL. For all of the control rats, none of the mean values of the sum of the amount of cerium in the organs or blood exceeded 1% of the nanoceria dose given to the paired nanoceria-treated rats.

Nine values from nanoceria-treated subjects were outliers by the Grubb's test. Of the 462 samples from nanoceria-treated rats analyzed for cerium, all but 56 (14%) were above the MDL; 20 were brain, 16 blood, and 15 were skeletal muscle samples, indicating the lowest nanoceria distribution into those organs.

There were no statistically significant differences in the percentage of the infused nanoceria dose between those rats that received a single dose and those that received 5 daily consecutive infusions of the same dose (Figure 3). The 6 mg/kg infusion of 30 nm ceria significantly increased cerium in most organs and blood. This is shown by the statistically significant differences compared to control rats and when all of the cerium levels in the control rats were below the MDL, leading to the inability to statistically compare results from control and nanoceria-treated rats (Figure 4). The only statistically significant decreases of cerium seen up to 90 days after infusion of 6 mg/kg of the 30 nm ceria were in the liver and skeletal muscle (Figure 4). One day after a single IV infusion of 6 mg/kg of the 30 nm ceria, 71% of the dose was in the liver. The percentage of the injected dose in the liver 90 days after the single IV infusion had decreased to 26% (Figure 4). Our prior results showed that less (33%) of an 85 mg/kg dose of the 30 nm ceria was in the liver 1 day after IV infusion compared to 71% of the 6 mg/kg dose. This decreased to 21% 90 days after the 85 mg/kg dose [31]. The reduction of 12% of the 85 mg/kg dose (from 33 to 21%) is 10.2 mg/kg. This is a greater reduction of cerium mass in the liver than the 45% reduction of the 8 mg/kg dose (from 71 to 26%), which is 3.6 mg/kg.

The ceria nanorod distribution was generally similar to the 5 and 30 nm cubic/polyhedral nanoceria of the present study and our prior results with this 5 and 30, as well as a 15 and 55 nm cubic ceria [31, 32] (Figure 5). There was no significant reduction of cerium levels at 30 days, compared to the first h, after the ceria nanorod infusion. In contrast, cerium increased in bone marrow and spleen, resulting in a greater percentage of the dose in these mononuclear phagocyte system (MPS) sites than most other nanoceria treatments we have studied (Figure 6).

Results of the relative deposition index show accumulation in liver within 1 h that persisted for 30 or 90 days for the 5 and 30 nm ceria, but not the ceria nanorod (Table 2). The accumulation in the bone marrow at 30 days and nanorod in the spleen at 30 days might represent uptake of nanoceria that was located in other sites, or dissolution of nanoceria and distribution of cerium to these sites.

The sum of the percentages of the ceria dose in the sampled blood and organs accounted for 70 and 72% of the single and repeated 5 nm ceria; 79, 56 and 36% of the 30 nm ceria at 1, 30 and 90 days; 53 and 78% for the 50 mg/kg ceria nanorod dose after 1 h and 30 days; and 49% for the 20 mg/kg ceria nanorod dose after 30 days. As appreciable fecal and urinary cerium excretion were not seen after systemic nanoceria administration [31, 33], the remainder of the dose was evidently in un-sampled sites, one of which appears to be adherence to the luminal wall of blood vessels [70].

Most of the nanoceria was cleared into MPS organs. When cerium was determined in only blood, brain, liver and spleen, with the exception of the first h after infusion of the 5 nm ceria when a significant amount was still in blood, ≥ 98% was in the liver and spleen. When bone marrow was also collected among 11 to 16 tissues and fluids, ≥ 88% was in the liver, spleen, and bone marrow, with the exception that these 3 MPS organs accounted for only 72% of the dose 90 days after the 85 mg/kg dose of 30 nm ceria [31]. The percentage of the dose in the liver decreased over time for the 6 mg/kg dose of 30 nm ceria, the ceria nanorod of the present study, and the 85 mg/kg dose of 30 nm ceria in our prior study [31] (Figure 6), suggesting some translocation out of the liver over time. Following the 85 mg/kg dose of the 30 nm ceria and the ceria nanorod, there was an increase in the spleen.

	5 nm		30 nm, 6 mg/kg			Nanorod		
	11 mg/kg, day 30	55 mg/kg, day 30	1 h	day 30	day 90	50 mg/kg, 1 h	20 mg/kg, day 30	50 mg/kg, day 30
Liver	X	X	X	X	X	X		
Bone marrow	X	X						X
Spleen	X		X	X	X		X	X

Table 2. Results of relative deposition index (RDI) analysis. X = organs showing both RDI > 1 and a partial chi-squared value for that organ representing > 10% of the sum of the partial chi-squared values.

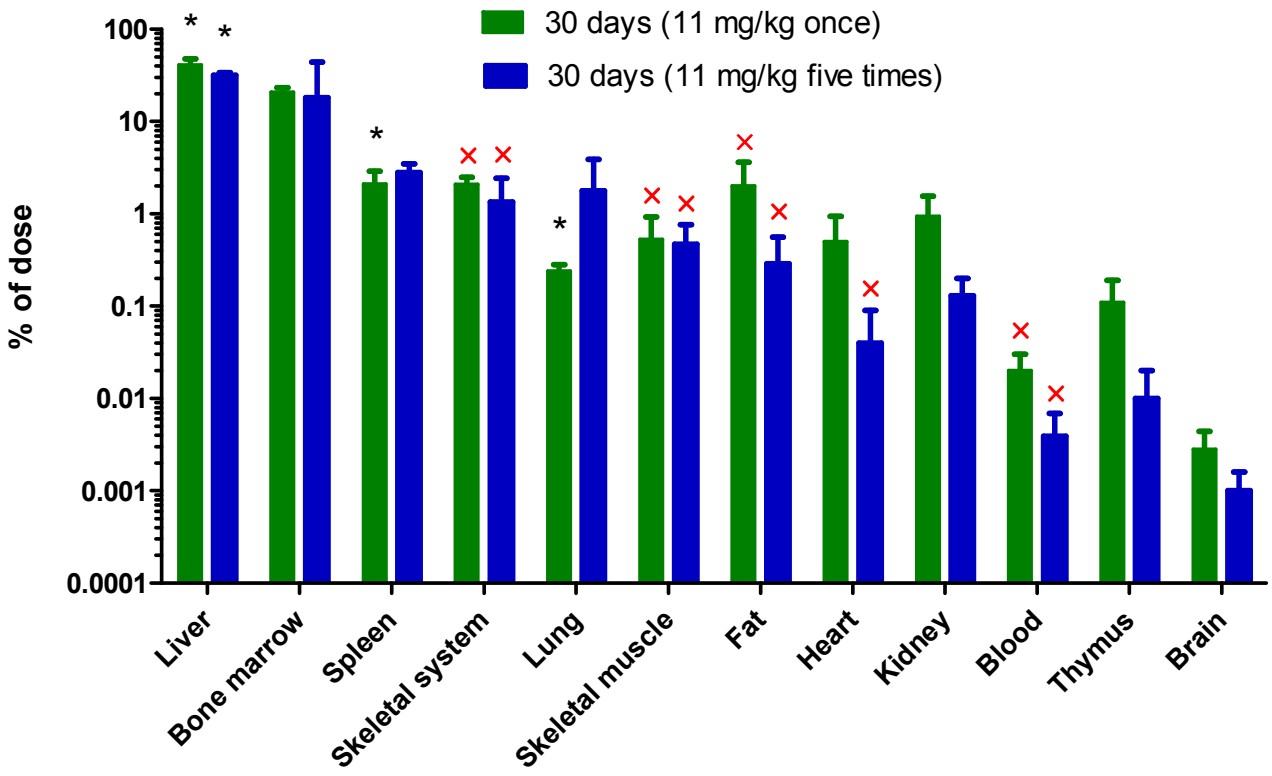

Figure 3. Percentage of the nanoceria dose in tissues and blood 30 days after one or five IV 11 mg/kg 5 nm ceria administrations.* = Significantly different from controls. × = Cannot test for significant difference from controls because all of the control rat values were identical (below the MDL).

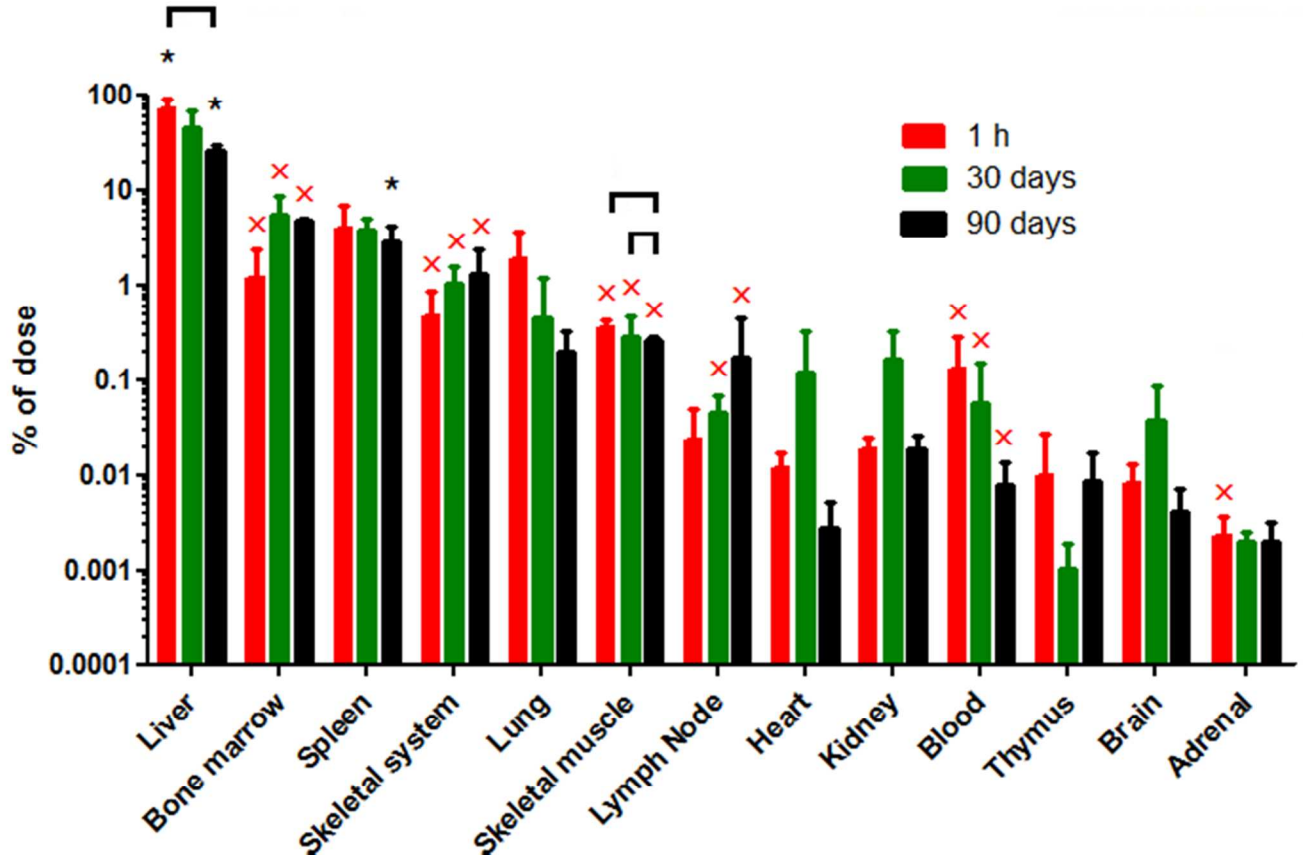

Figure 4. Percentage of the nanoceria dose in tissues and blood after a single IV 6 mg/kg 30 nm ceria administration.* = Significantly different from controls. × = Cannot test for significant difference from controls because all of the control rat values were identical (below the MDL). ∏ indicates a statistically significant difference between the two treatments.

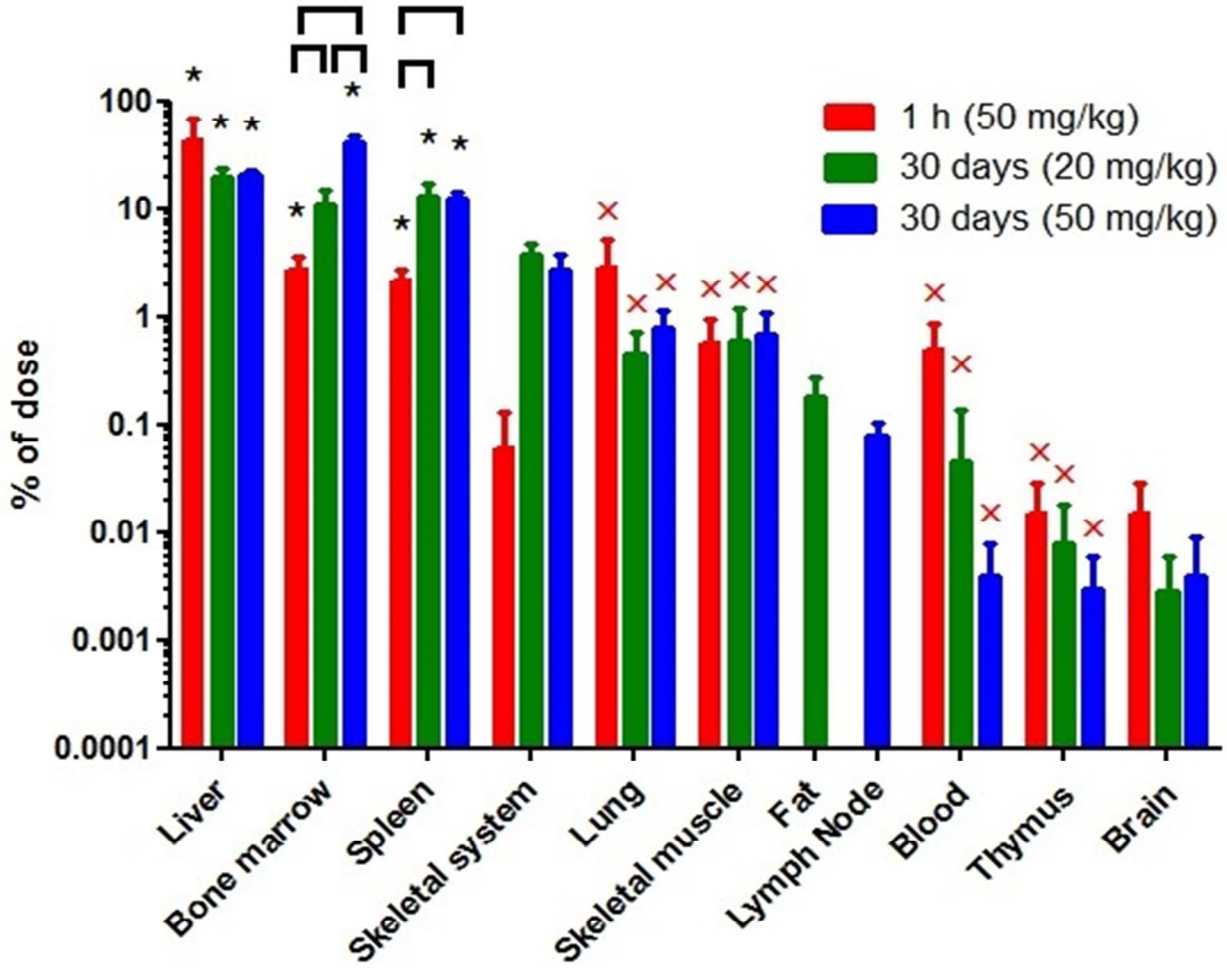

Figure 5. Percentage of the nanoceria dose in tissues and blood after a single IV ceria nanorod administration. * = Significantly different from controls. × = Cannot test for significant difference from controls because all of the control rat values were identical (below the MDL). ∏ indicates a statistically significant difference between the two treatments.

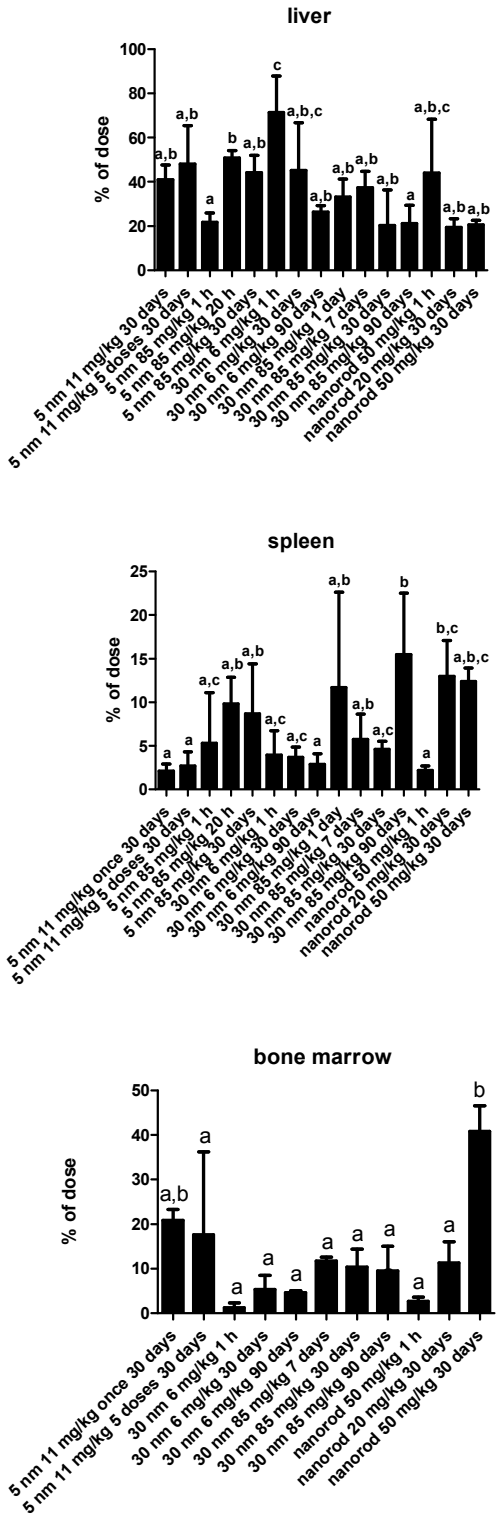

Figure 6. Percentage of the nanoceria dose in the liver, spleen, and bone marrow of the current study and prior studies of 5 and 30 nm ceria, 85 mg/kg [31, 32]. Treatments that have a common letter are not statistically different.

Discussion:

The aims of these studies were to determine if the biodistribution and persistence of nanocerias are different following lower doses than we previously studied; if repeated dosing influences its disposition; and if the nanoceria shape has a significant influence on its toxicity, disposition and retention. Overall, the results suggest that these three variables do not have a profound effect on the biodistribution or persistence of nanocerias, e.g., the distribution and fate of these representative nanoceria, and others we have studied is more similar than different (Figure 6). Each of the nanoceria doses significantly increased cerium in multiple organs and blood. Overall, 85% of the samples, including those collected 90 days after the single nanoceria administration, were above the MDL.

In contrast, only 20% of the samples from non-nanoceria-treated rats were above the MDL of this highly sensitive analytical method. Control rat samples above the MDL were most commonly from the liver, spleen, brain, bone marrow, bone, and lung, suggesting the greatest accumulation of cerium from dietary and other sources in these organs. Cerium is the most abundant of the rare earth elements, comprising ~ 0.005% of the Earth's crust; more than lead, silver, mercury, or gold. Its oral bioavailability is very low. After oral introduction, only 0.03% was absorbed from the gastrointestinal tract of rats within 3 days [71]. It was reported to accumulate principally in muscle [72], bone [73-75], and liver [75, 76] after oral administration to various mammals. Cerium concentration in healthy adult Chinese men who suffered sudden death was 90, 58, and 36 μg/kg in liver, lung, and rib, respectively; 5 to 10 in pancreas, skin and thymus; 1 to 5 in adrenals, fat, heart, kidney, large and small intestine, muscle, spleen, stomach, testis, and thyroid; and < 1 in blood [77], consistent with the pattern of cerium in the control rats that did not receive nanoceria.

The rats in this work were not perfused to remove blood from their organs when terminated, because we needed to quickly harvest tissues, unaltered, for determination of biochemical endpoints. Based on the rat brain vascular volume (2% of the frontal cortex and 2.6% of gray matter) [78] and cerium concentration in blood determined in this study, the cerium in the brain of these nanoceria-treated rats can be accounted for by the cerium in circulating blood. Our previous attempts to visualize nanoceria in brain parenchyma after IV infusion of 5 and 30 nm ceria revealed very few nanoceria particles had crossed the blood-brain barrier [30-32, 47, 48]. Therefore, these results provide no evidence that these nanoceria distributed into brain parenchyma. After a much smaller dose of nanoceria administered by the oral, intraperitoneal, and IV routes (0.5 mg/kg), cerium could not be detected in the brain of mice [33]. A small percentage of oral and intratracheal doses of nanoceria was shown by ICP-MS analysis to be in brain, but techniques, such as electron microscopy, were not utilized to determine its location [28]. These results are in contrast to results with a citrate-EDTA stabilized 2.9 nm ceria that appears to result in significant accumulation in the cerebellum of mice with experimental autoimmune encephalomyelitis [19].

Intravenous administration of 50 to 750 mg/kg of a 30 nm commercial (platelet shaped) ceria resulted in 57, 16, and 0.01-0.02% of the dose in the liver, spleen, and brain, respectively, 20 h later [30]. After a single infusion of 50 to 85 mg/kg of 5, 15, or 30 nm ceria, liver had the greatest percentage of the administered dose (44, 23, and 33%) 30 days later [32]. Spleen

nanoceria concentrations were ~ 2, 5, and 4-fold greater than in the liver; containing 9, 15, and 11% of the dose for those 3 nanoceria sizes, respectively. Similarly, liver, spleen, and bone marrow contained a greater percentage of the dose of a 30 nm ceria 90 days after an 85 mg/kg IV dose (21, 15 and 9.5%) than did 12 other organs, blood, or cerebrospinal fluid [31]. The present results also show considerable uptake by MPS organs within 1 h. These nanoceria are too large to be excreted by the kidney. Previous results show little of the 30 nm ceria was excreted in urine or feces, consistent with their prolonged residence in the body [31]. There was little uptake into the lungs, suggesting the circulating, rigid, nanoceria had not agglomerated to particles in the μm range, that would be cleared from systemic circulation into the lung [79], consistent with our observation that nanoceria agglomerations were < 1 μm after 1 h *ex vivo* incubation of a 30 nm ceria in blood [30]. The result of studies with five nanoceria with primary particles sizes from 3 to 40 nm show < 1 is taken up into distal organs from the lungs (after intratracheal instillation and nose-only inhalation) and much less than 1% from the GI tract. The distribution pattern of the cerium in distal organs after pulmonary, oral, or IP introduction was generally similar to the present pattern following IV injection [28, 33, 35, 80]. Furthermore, the cerium distribution pattern following IV infusion of nanoceria is similar to other nanoscale materials, including colloidal carbon [81], colloidal gold [82, 83], other quite insoluble metal oxides [84-88], and polymeric nanomaterials [89, 90] , although not generally as extensively described in those studies as for nanoceria in the present studies.

Cerium in the skeletal system increased from 1 h to 30 and 90 days after nanoceria injection (Figures 4 and 5). Cerium in cranium, spinal column, pelvis, or femur did not decrease from 1 to 90 days after IV injection of 85 mg/kg of the 30 nm ceria [31]. Given the concentration of cerium in the ribs of healthy adult Chinese men who suffered sudden death compared to other organs (summarized above), and relative organ weights, they had more cerium in their skeletal systems than any other sampled organ [77]. Similarly, after SC, IM, or IV cerium injection, there was more cerium in rat's skeleton than liver 15 days later [62]. Bone might be a major, persistent, depot of cerium accumulation after nanoceria exposure.

The only significant decrease of cerium up to 90 days after infusion of 6 mg/kg 30 nm ceria was in the liver and skeletal muscle (Figure 4). A reduction in liver cerium was also seen after its IV injection into rats over 5 months [19]. These results further illustrate the persistence of cerium in MPS organs we saw with higher doses [30-32]. The reduction of cerium in the liver over time and its increase in some other sites suggests translocation. The percent of the dose in the spleen increased over time after infusion of 15 and 30 nm ceria [32]. Although considered to be quite insoluble, there is evidence for some dissolution of nanoceria in plants [91], and *in vivo* over months [51]. This may be associated with nanoceria reduction in the liver and increase in cerium in other sites, and might account for the increase in cerium at several sites 90 days after the single infusion of 85 mg/kg 30 nm ceria [31]. The greater reduction in the liver of the mass amount of the 30 nm ceria dose after the 85 than the 6 mg/kg administration suggests the mechanism mediating nanoceria clearance from the liver was not saturated after the higher dose.

A close review of the results shown in Figure 6 suggests there are some trends. In the presence of the highest dose tested, 85 mg/kg, a lower percentage enters the liver than at lower doses, suggesting an initial saturation of the liver's ability to clear nanoceria from blood. Larger nanoceria doses result in a greater percentage taken up by the bone marrow. Higher dose ceria nanorod administration results in greater bone marrow uptake than after the 5 and 30 nm ceria.

The stability of this ceria nanorod was evaluated by measuring its crystallography (XRD) and hydrodynamic diameter of two samples stored for three years. The dried powder gave an XRD pattern essentially identical to Figure 2, confirming excellent stability when stored in a dry state. Other researchers reported nanorods with high fractions of (200) morphology, which would lead to high oxygen vacancies and/or high Ce^{3+} content [92, 93]. This ceria nanorod appears to have a lower (200) content than these reports. The DLS data shown in Table 1 were taken on a suspension of our nanoceria in 10% sucrose, stored for three years and sonicated briefly after 100:1 dilution. DLS data analysis techniques are normally based on the assumption of spheroidal geometer; no correction was made based on the cylindrical morphology of the nanorods. The 1st peak, centered around 100 nm, likely corresponds to discrete, unagglomerated nanorods (expected to have a size between the volume-equivalent diameter of a sphere the same volume as the nanorods (34 nm) and the nanorod average length, 264 nm). The 2nd peak, centered around 400 nm, likely corresponds to agglomerated nanorods.

The ceria nanorod was not much more acutely toxic than the cubic/polyhedral nanoceria. Work with carbon nanotubes having a length less than 1 μm showed them to have apparent *in vivo* bio-compatibility and minimal cytotoxicity [94]. Increasing the aspect ratio has been found to increase the rate of cell entry [95]. Thirteen to 20 nm diameter, 100 to 300 nm length, and 5 to 10 nm diameter, 25 to 35 nm length ceria nanorods were more catalytically active than 8 nm irregularly shaped ceria [96, 97]. To investigate the influence of length and aspect ratio of nanorods on biological activity, a library of 6 to 10 nm diameter, 31 to > 1000 nm length, ceria nanorods was prepared [98]. They were taken up into the cytoplasm and membrane-lined compartments of THP-1 (human monomyelocytic leukemia) cells. Cytotoxicity, as LDH release, and IL-1β (which has been shown to play a role in the generation of chronic granulomatous inflammation and fibrosis by multiwalled carbon nanotubes) were much greater in THP-1 cells exposed to the 500 and >1000 nm ceria nanorods than the shorter ones. NALP3 inflammasome-mediated lysosomal damage was seen. This investigation was extended into the mouse (oropharyngeal aspiration) and zebrafish larvae (immersion) which yielded similar results of increased toxicity as length increased, particularly when length was ≥ 500 nm [99]. The high tolerated dose of nanorod ceria in the present work is consistent with the lack of significant toxicity of nanorods with lengths below 500 nm. The inverse correlation between ceria nanorod diameter and length was expected, based on work with multi-walled carbon nanotubes [100]. Nanotubes with greater diameter are stiffer therefore fracture more easily as one would predict based on the radius of curvature prior to fracturing. The low correlation between diameter and length for the ceria nanorods in this study can be attributed to the fairly narrow diameter variability.

The nanoceria in the present work were citrate coated. Others have studied crystalline 3 to 5 nm primary ceria particles functionalized with carboxyfluorescein [33], 5 nm ceria functionalized with 3-aminopropylsilyl-anchored N-succinimidyl 4-[^{18}F]fluorobenzoate

[101], and 2.9 nm citrate-EDTA stabilized ceria [19] and found similar distribution after IV administration. These results suggest the surface coating of nanoceria does not greatly influence its biodistribution.

In summary, cerium determined in ~ 12 organs and tissues from 1 h to 90 days after IV infusion of a 5 nm polyhedral, a 30 nm cubic nanoceria, and a ceria nanorod was mainly in MPS organs, with no evidence of entry into brain parenchyma. There was little decrease in the percent of the nanoceria dose in the rat for up to 90 days, although there was a decrease in the liver and increase in some other sites, suggesting some translocation or nanoceria dissolution and cerium redistribution.

Conclusions

Investigation of the distribution and persistence of a repeatedly-dosed 5 nm nanoceria, a 30 nm ceria given as a > 10-fold lower dose than we previously studied, and an ~ 10 x 265 nm ceria nanorod, when compared to prior reports of nanoceria distribution and persistence with various nanoceria with different surface coatings, suggests some trends. Higher doses resulted in a greater percentage uptake by the spleen and bone marrow. Overall, these results show greater similarity than difference in the fate of nanocerias, helping to unify and simply our understanding of the handling of nanocerias by mammalian organisms.

Acknowledgements

The authors thank Hamed Haghnazar for his contribution to this research and Matt Hazzard for creating the colour graphic. This work was supported by United States Environmental Protection Agency Science to Achieve Results [grant number RD-833772]. Although the research described in this article has been funded wholly or in part by the United States Environmental Protection Agency through STAR Grant RD-833772, it has not been subjected to the Agency's required peer and policy review and therefore does not necessarily reflect the views of the Agency and no official endorsement should be inferred.

Notes and references

[a] Pharmaceutical Sciences, University of Kentucky.
[b] Graduate Center for Toxicology, University of Kentucky.
[c] Plant and Soil Sciences, University of Kentucky.
[d] Chemical & Materials Engineering, University of Kentucky.

Abbreviations:

ICP-MS	inductively coupled plasma mass spectrometry
MDL	method detection limit
MPS	mononuclear phagocyte system

1. K. Reed, A. Cormack, A. Kulkarni, M. Mayton, D. Sayle, B. Stadler and F. Klaessig, *Environ. Sci.: Nano,* 2014, 1, DOI: 10.1039/C4EN00079J.
2. N. Singh, C. A. Cohen and B. A. Rzigalinski, *Ann. N. Y. Acad. Sci.*, 2007, **1122**, 219-230.
3. J. M. Perez, A. Asati, S. Nath and C. Kaittanis, *Small*, 2008, **4**, 552-556.
4. S.-g. Shen, H.-l. Liu, W.-y. Wang, G.-q. Gu and G.-q. Zhou, *Hebei Daxue Xuebao, Ziran Kexueban*, 2011, **31**, 160-166.
5. F. Pagliari, C. Mandoli, G. Forte, E. Magnani, S. Pagliari, G. Nardone, S. Licoccia, M. Minieri, N. P. Di and E. Traversa, *ACS Nano*, 2012, **6**, 3767-3775.
6. A. B. Shcherbakov, N. M. Zholobak, V. K. Ivanov, O. S. Ivanova, A. V. Marchevsky, A. E. Baranchikov, N. Y. Spivak and Y. D. Tretyakov, *Russ. J. Inorg. Chem.*, 2012, **57**, 1411-1418.
7. T. Xia, M. Kovochich, M. Liong, L. Madler, B. Gilbert, H. Shi, J. I. Yeh, J. I. Zink and A. E. Nel, *ACS Nano*, 2008, **2**, 2121-2134.
8. R. W. Tarnuzzer, J. Colon, S. Patil and S. Seal, *Nano Letters*, 2005, **5**, 2573-2577.
9. J. Colon, L. Herrera, J. Smith, S. Patil, C. Komanski, P. Kupelian, S. Seal, D. W. Jenkins and C. H. Baker, *Nanomedicine*, 2009, **5**, 225-231.
10. J. Colon, N. Hsieh, A. Ferguson, P. Kupelian, S. Seal, D. W. Jenkins and C. H. Baker, *Nanomedicine*, 2010, **6**, 698-705.
11. D. Schubert, R. Dargusch, J. Raitano and S. W. Chan, *Biochem. Biophys. Res. Commun.*, 2006, **342**, 86-91.
12. B. D'Angelo, S. Santucci, E. Benedetti, S. Di Loreto, R. A. Phani, S. Falone, F. Amicarelli, M. P. Ceru and A. Cimini, *Curr. Nanoscience*, 2009, **5**, 167-176.
13. A. Y. Estevez, S. Pritchard, K. Harper, J. W. Aston, A. Lynch, J. J. Lucky, J. S. Ludington, P. Chatani, W. P. Mosenthal, J. C. Leiter, S. Andreescu and J. S. Erlichman, *Free Radical Biol. Med,*. 2011, **51**, 1155-1163.
14. S. M. Hirst, A. S. Karakoti, R. D. Tyler, N. Sriranganathan, S. Seal and C. M. Reilly, *Small*, 2009, **5**, 2848-2856.
15. J. Niu, K. Wang and P. E. Kolattukudy, *J. Pharmacol. Exp. Ther.*, 2011, **338**, 53-61.
16. A. Clark, A. Zhu, K. Sun and H. R. Petty, *J. Nanopart. Res.*, 2011, **13**, 5547-5555.
17. M. Das, S. Patil, N. Bhargava, J. F. Kang, L. M. Riedel, S. Seal and J. J. Hickman, *Biomaterials*, 2007, **28**, 1918-1925.
18. X. Zhou, L. L. Wong, A. S. Karakoti, S. Seal and J. F. McGinnis, *PLoS One*, 2011, **6**, e16733.
19. K. L. Heckman, W. DeCoteau, A. Estevez, K. J. Reed, W. Costanzo, D. Sanford, J. C. Leiter, J. Clauss, K. Knapp, C. Gomez, P. Mullen, E. Rathbun, K. Prime, J. Marini, J. Patchefsky, A. S. Patchefsky, R. K. Hailstone and J. S. Erlichman, *ACS Nano*, 2013, **7**, 10582-10596.
20. J. Niu, A. Azfer, L. M. Rogers, X. Wang and P. E. Kolattukudy, *Cardiovas. Res.*, 2007, **73**, 549-559.
21. M. B. Kolli, Marshall Univ., 2012, 147 pages.
22. S. Giri, A. Karakoti, R. P. Graham, J. L. Maguire, C. M. Reilly, S. Seal, R. Rattan and V. Shridhar, *PLoS ONE*, 2013, **8**, e54578.
23. M. S. Wason, J. Colon, S. Das, S. Seal, J. Turkson, J. Zhao and C. H. Baker, *Nanomedicine*, 2013, **9**, 558-569.
24. C. K. Kim, T. Kim, I.-Y. Choi, M. Soh, D. Kim, Y.-J. Kim, H. Jang, H.-S. Yang, J. Y. Kim, H.-K. Park, S. P. Park, S. Park, T. Yu, B.-W. Yoon, S.-H. Lee and T. Hyeon, *Angewandte Chemie Int. Ed.*, 2012, **51**, 11039-11043.
25. A. Arya, N. K. Sethy, S. K. Singh, M. Das and K. Bhargava, *Int. J. Nanomed.*, 2013, **8**, 4507-4520.
26. L. P. Babenko, N. M. Zholobak, A. B. Shcherbakov, S. I. Voychuk, L. M. Lazarenko and M. Y. Spivak, *Mikrobiol. Z.*, 2012, **74**, 54-62.
27. Q. Wang, J. M. Perez and T. J. Webster, *Int. J. Nanomed.*, 2012, **8**, 3395-3399.
28. X. He, H. Zhang, Y. Ma, W. Bai, Z. Zhang, K. Lu, Y. Ding, Y. Zhao and Z. Chai, *Nanotechnology*, 2010, **21**, 285103/285101-285103/285108.
29. W.-S. Cho, R. Duffin, F. Thielbeer, M. Bradley, I. L. Megson, W. Macnee, C. A. Poland, C. L. Tran and K. Donaldson, *Toxicol. Sci.*, 2012, **126**, 469-477.
30. R. A. Yokel, R. L. Florence, J. M. Unrine, M. T. Tseng, U. M. Graham, P. Wu, E. A. Grulke, R. Sultana, S. S. Hardas and D. A. Butterfield, *Nanotoxicology*, 2009, **3**, 234-248.
31. R. A. Yokel, T. C. Au, R. MacPhail, S. S. Hardas, D. A. Butterfield, R. Sultana, M. T. Tseng, M. Dan, R. L. Florence, J. M. Unrine, U. M. Graham, P. Wu and E. A. Grulke, *Toxicol. Sci.*, 2012, **127**, 256-268.
32. R. A. Yokel, M. T. Tseng, M. Dan, J. M. Unrine, U. M. Graham, P. Wu and E. A. Grulke, *Nanomedicine: Nanotechnology, Biology, and Medicine*, 2013, **9**, 398-407.
33. S. M. Hirst, A. Karakoti, S. Singh, W. Self, R. Tyler, S. Seal and C. M. Reilly, *Environ. Toxicol.*, 2011, 1-12.

34. L. L. Wong, S. M. Hirst, Q. N. Pye, C. M. Reilly, S. Seal and J. F. McGinnis, *PLoS ONE*, 2013, **8**, e58431.
35. E.-J. Park, Y.-K. Park and K. Park, *Toxicol. Res.*, 2009, **25**, 79-84.
36. T. J. Brunner, P. Wick, P. Manser, P. Spohn, R. N. Grass, L. K. Limbach, A. Bruinink and W. J. Stark, *Environ. Sci. Technol.*, 2006, **40**, 4374-4381.
37. E. J. Park, J. Choi, Y. K. Park and K. Park, *Toxicology*, 2008, **245**, 90-100.
38. H. J. Eom and J. Choi, *Toxicol. Lett.*, 2009, **187**, 77-83.
39. E.-J. C. Park, Wan-Seob, J. Jeong, J.-h. Yi, K. Choi, Y. Kim and K. Park, *J. Health Sci.*, 2010, **56**, 387-396.
40. A. Srinivas, P. J. Rao, G. Selvam, P. B. Murthy and P. N. Reddy, *Toxicol. Lett.*, 2011, **205**, 105-115.
41. J. Y. Ma, R. R. Mercer, M. Barger, D. Schwegler-Berry, J. Scabilloni, J. K. Ma and V. Castranova, *Toxicol. Appl. Pharmacol.*, 2012, **262**, 255-264.
42. J. Y. Ma, H. Zhao, R. R. Mercer, M. Barger, M. Rao, T. Meighan, D. Schwegler-Berry, V. Castranova and J. K. Ma, *Nanotoxicology*, 2011, **5**, 312-325.
43. V. C. Minarchick, P. A. Stapleton, D. W. Porter, M. G. Wolfarth, E. Ciftyurek, M. Barger, E. M. Sabolsky and T. R. Nurkiewicz, *Cardiovasc. Toxicol.*, 2013, **13**, 323-337.
44. M. T. Tseng, X. Lu, X. Duan, S. S. Hardas, R. Sultana, P. Wu, J. M. Unrine, U. M. Graham, D. A. Butterfield, E. A. Grulke and R. A. Yokel, *Toxicol. Appl. Pharmacol.*, 2012, **260**, 173-182.
45. M. T. Tseng, Fu, Q., G. K. Lorc, R. Fernandez-Botran, Z.-B. Deng, U. M. Graham, D. A. Butterfield, E. A. Grulke and R. A. Yokel, *Toxicologic Pathol.*, 2014, **42**, 984-996.
46. S. K. Nalabotu, M. B. Kolli, W. E. Triest, J. Y. Ma, N. D. Manne, A. Katta, H. S. Addagarla, K. M. Rice and E. R. Blough, *Int J Nanomedicine*, 2011, **6**, 2327-2335.
47. S. S. Hardas, D. A. Butterfield, R. Sultana, M. T. Tseng, M. Dan, R. L. Florence, J. M. Unrine, U. M. Graham, P. Wu, E. A. Grulke and R. A. Yokel, *Toxicol. Sci.*, 2010, **116**, 562-576.
48. S. S. Hardas, R. Sultana, G. Warrier, M. F. Dan, R.L., P. Wu, E. A. Grulke, M. T. Tseng, J. M. Unrine, U. M. Graham, R. A. Yokel and D. A. Butterfield, *Neurotoxicology*, 2012, **33**, 1147-1155.
49. S. S. Hardas, R. Sultana, G. Warrier, M. Dan, P. Wu, E. A. Grulke, M. T. Tseng, J. M. Unrine, U. M. Graham, R. A. Yokel and D. A. Butterfield, *Nanotoxicology*, 2014, **8**, 155-166.
50. A. S. Karakoti, N. A. Monteiro-Riviere, R. Aggarwal, J. P. Davis, R. J. Narayan, W. T. Self, J. McGinnis and S. Seal, *JOM*, 2008, **60**, 33-37.
51. U. M. Graham, M. T. Tseng, J. B. Jasinski, R. A. Yokel, J. M. Unrine, B. H. Davis, A. K. Dozier, S. S. Hardas, R. Sultana, E. Grulke and D. A. Butterfield, *ChemPlusChem*, 2014, **79**, 1083-1088.
52. S. Park, N. Sinha and K. Hamad-Schifferli, *Langmuir*, 2010, **26**, 13071-13075.
53. H.-X. Mai, L.-D. Sun, Y.-W. Zhang, R. Si, W. Feng, H.-P. Zhang, H.-C. Liu and C.-H. Yan, *J. Phys. Chem. B* 2005, **109**, 24380-24385.
54. B. Wang, P. Wu, R. A. Yokel and E. A. Grulke, *Appl. Surf. Sci.*, 2012, **258**, 5332-5341.
55. R. J. Probst, J. M. Lim, D. N. Bird, G. L. Pole, A. K. Sato and J. R. Claybaugh, *J. Am. Assoc. Lab. Animal Sci.*, 2006, **45**, 49-52.
56. A. G. Sanders and H. W. Florey, *Brit. J. Exp Path.*, 1940, **21**, 275-287.
57. A. Yamashita, T. Fukumoto and M. Miyamoto, *Immunology*, 1976, **30**, 349-359.
58. M. J. Manning, *J. Endocrinol.*, 1959, **19**, 143-149.
59. H. Nagata, T. Arai, Y. Soejima, H. Suzuki, H. Ishii and T. Hibi, *Cancer Res.*, 2004, **64**, 8239-8248.
60. E. Fairman and G. W. Corner, *Anatomical Record*, 1934, **60**, 1-4.
61. S. Schermer, *The blood morphology of laboratory animals*, 3 edn., F. A. Davis Company, Philadelphia, PA, 1967.
62. K. Takada and M. Fujita, *J. Radiat. Res. (Tokyo)*, 1973, **14**, 187-197.
63. T. Soukup, G. Zacharova, V. Smerdu and I. Jirmanova, *Physiol. Res.*, 2001, **50**, 619-626.
64. R. Schemmel, O. Mickelsen and J. L. Gill, *J. Nutr.*, 1970, **100**, 1041-1048.
65. D. J. Schoeffner, D. A. Warren, S. Muralidara, J. V. Bruckner and J. E. Simmons, *J. Toxicol. Environ. Health A*, 1999, **56**, 449-462.
66. B. S. Halilu, J. S. Keller and J. Bujko, *Z. Ernaehrungswissenschaft* 1997, **36**, 321.
67. C. Mühlfeld, T. M. Mayhew, P. Gehr and B. Rothen-Rutishauser, *J. Aerosol Med.*, 2007, **20**, 395-407.
68. M. Geiser, O. Quaile, A. Wenk, C. Wigge, S. Eigeldinger-Berthou, S. Hirn, M. Schäffler, C. Schleh, W. Möller, M. A. Mall and W. G. Kreyling, *Part. Fibre Toxicol.*, 2013, **10**, 19.
69. V. Kanniah, B. Wang, Y. Yang and E. A. Grulke, *J. Appl. Polymer Sci.*, 2012, **125**, 165-174.
70. M. Dan, M. T. Tseng, P. Wu, J. M. Unrine, E. A. Grulke and R. A. Yokel, *Int. J. Nanomed,*. 2012, **7**, 4023-4036.
71. Y. I. Moskalev, *Meditsinskaya Radiologiya*, 1959, **4**, 52-57.
72. R. Tang, W. Huang, G. Xiao and Y. Liu, *Tongweisu*, 1991, **4**, 71-75.
73. K. V. Grigoryan, *Raspred. Biol. Deistvie Radioakt. Izot.*, 1966, 50-55.
74. F. R. Mraz and G. R. Eisele, *Health Phys.*, 1977, **33**, 494-495.
75. L. A. Buldakov, *Biol. Deistvie Radiatsii i Vopr. Raspredeleniya Radioaktivn. Izotopov, Sb. Rabot*, 1961, 70-79.
76. J. K. Miller and W. F. Byrne, *J. Dairy Sci.*, 1970, **53**, 171-175.
77. H. D. Zhu, J. Y. Wang, Q. Wu, N. F. Wang, T. J. Fan, H. S. Liu, Q. F. Liu, X. Y. Wang, L. Ou-Yang, Y. Q. Liu and Q. Xie, *Chin. Med. Sci. J.*, 2007, **22**, 71-82.
78. K. Ohno, K. D. Pettigrew and S. I. Rapoport, *Am. J. Physiol.*, 1978, **235**, H299-H307.
79. T. J. Merkel, S. W. Jones, K. P. Herlihy, F. R. Kersey, A. R. Shields, M. Napier, J. C. Luft, H. Wu, W. C. Zamboni, A. Z. Wang, J. E. Bear and J. M. DeSimone, *Proc. Natl. Acad. Sci. U. S. A.*, 2011, **108**, 586-591, S586/581-S586/586.
80. L. Geraets, A. G. Oomen, J. D. Schroeter, V. A. Coleman and F. R. Cassee, *Toxicol. Sci.*, 2012, **127**, 463-473.
81. S. Takahashi and O. Matsuoka, *J. Toxicol. Sci.*, 1980, **5**, 215-223.
82. N. Gheorghe, *Rev. Roum. Physiol.*, 1972, **9**, 145-150.
83. J. M. Singer, L. Adlersberg and M. Sadek, *RES J. Reticuloendothel. Soc.*, 1972, **12**, 658-671.
84. N. Shinohara, N. Danno, T. Ichinose, T. Sasaki, H. Fukui, K. Honda and M. Gamo, *Nanotoxicology*, 2014, **8**, 132-141.
85. D. K. Tiwari, T. Jin and J. Behari, *Int. J. Nanomed.*, 2011, **6**, 463-475.
86. S. Hirn, M. Semmler-Behnke, C. Schleh, A. Wenk, J. Lipka, M. Schaffler, S. Takenaka, W. Moller, G. Schmid, U. Simon and W. G. Kreyling, *Eur. J. Pharm. Biopharm.*, 2011, **77**, 407-416.
87. T. Baati, L. Njim, F. Neffati, A. Kerkeni, M. Bouttemi, R. Gref, M. F. Najjar, A. Zakhama, P. Couvreur, C. Serre and P. Horcajada, *Chem. Sci.*, 2013, **4**, 1597-1607.
88. E. Fabian, R. Landsiedel, L. Ma-Hock, K. Wiench, W. Wohlleben and B. van Ravenzwaay, *Arch. Toxicol.*, 2008, **82**, 151-157.
89. Y. Wenger, R. J. Schneider, II, G. R. Reddy, R. Kopelman, O. Jolliet and M. A. Philbert, *Toxicol. Appl. Pharmacol.*, 2011, **251**, 181-190.
90. A. Ambruosi, H. Yamamoto and J. Kreuter, *J. Drug Targeting*, 2005, **13**, 535-542.
91. P. Zhang, Y. Ma, Z. Zhang, X. He, J. Zhang, Z. Guo, R. Tai, Y. Zhao and Z. Chai, *ACS Nano*, 2012, **6**, 9943-9950.
92. S. Turner, S. Lazar, B. Freitag, R. Egoavil, J. Verbeeck, S. Put, Y. Strauven and G. Van Tendeloo, *Nanoscale*, 2011, **3**, 3385-3390.
93. E. Aneggi, D. Wiater, C. de Leitenburg, J. Llorca and A. Trovarelli, *ACS Catalysis*, 2014, **4**, 172-181.
94. V. Raffa, O. Vittorio, C. Riggio and A. Cuschieri, *Minim. Invasive. Ther. Allied Technol.*, 2010, **19**, 127-135.
95. S. E. Gratton, P. A. Ropp, P. D. Pohlhaus, J. C. Luft, V. J. Madden, M. E. Napier and J. M. DeSimone, *Proc. Natl. Acad. Sci. U S A*, 2008, **105**, 11613-11618.
96. K. Zhou, X. Wang, X. Sun, Q. Peng and Y. Li, *J. Catal.*, 2005, **229**, 206-212.
97. C. Pan, D. Zhang, L. Shi and J. Fang, *Eur. J. Inorg. Chem.*, 2008, 2429-2436.
98. Z. Ji, X. Wang, H. Zhang, S. Lin, H. Meng, B. Sun, S. George, T. Xia, A. E. Nel and J. I. Zink, *ACS Nano*, 2012, **6**, 5366-5380.

99. S. Lin, X. Wang, Z. Ji, C. H. Chang, Y. Dong, H. Meng, Y.-P. Liao, M. Wang, T.-B. Song, S. Kohan, T. Xia, J. I. Zink, S. Lin and A. E. Nel, *ACS Nano*, 2014, Ahead of Print.
100. J. Hilding, E. A. Grulke, Z. G. Zhang and F. Lockwood, *J. Dispersion Sci. Technol.*, 2003, **24**, 1-41.
101. S. Rojas, J. D. Gispert, S. Abad, M. Buaki-Sogo, V. M. Victor, H. Garcia and J. R. Herance, *Mol. Pharmaceut.*, 2012, **9**, 3543-3550.

Nanoceria distribution and retention in the rat is not greatly affected by its dose, size, shape, or dosing schedule.